Synthesis and Antitumor Activity of Stearate-*g*-dextran Micelles for Intracellular Doxorubicin Delivery

Yong-Zhong Du,* Qi Weng, Hong Yuan, and Fu-Qiang Hu

College of Pharmaceutical Sciences, Zhejiang University, 388 Yuhangtang Road, Hangzhou 310058, P.R. China

ABSTRACT Stearate-*g*-dextran (Dex-SA) was synthesized *via* an esterification reaction between the carboxyl group of stearic acid (SA) and hydroxyl group of dextran (Dex). Dex-SA could self-assemble to form nanoscaled micelles in aqueous medium. The critical micelle concentration (CMC) depended on the molecular weight of Dex and the graft ratio of SA, which ranged from 0.01 to 0.08 mg mL^{-1}. Using doxorubicin (DOX) as a model drug, the drug encapsulation efficiency (EE%) using Dex-SA with 10 kDa molecular weight of Dex and 6.33% graft ratio of SA could reach up to 84%. *In vitro* DOX release from DOX-loaded Dex-SA micelles (Dex-SA/DOX) could be prolonged to 48 h, and adjusted by a different molecular weight of Dex, the graft ratio of SA, or the drug-loading content. Tumor cellular uptake test indicated that Dex-SA micelles had excellent internalization ability, which could deliver DOX into tumor cells. *In vitro* cytotoxicity tests demonstrated the Dex-SA/DOX micelles could maintain the cytotoxicity of commercial doxorubicin injection against drug-sensitive tumor cells. Moreover, Dex-SA/DOX micelles presented reversal activity against DOX-resistant cells. *In vivo* antitumor activity results showed that Dex-SA/DOX micelles treatments effectively suppressed the tumor growth and reduced the toxicity against animal body compared with commercial doxorubicin injection.

KEYWORDS: dextran · stearic acid · polymeric micelles · doxorubicin · antitumor activity · drug resistance

In the last two decades, polymeric micelles with core—shell structure have attracted considerable interest especially for delivering antitumor drugs to solid tumors, which could be self-assembled from amphiphilic block or graft copolymers. Polymeric micelles with nano-order size have many advantages, such as the accumulation in tumor *via* the passive "enhanced permeability and retention (EPR) effect".[1,2] The hydrophilic surface allows avoiding reticuloendothelial system (RES) uptake, which helps to increase blood residence time.[3] Through chemical conjugation or physical entrapment, poorly water-soluble drugs can be incorporated into micelles with the purpose of solubilizing drugs and avoiding the use of some excipients such as Cremophor EL which easily causes hypersensitivity reactions.[4−10]

Materials used for preparing micelles for drug delivery should be biocompatible such as polycaprolactone, polysaccharides, poly-(acrylic acid) family, proteins or polypeptides. Among them, polysaccharides are the most popular recently because of their biocompatibility, biodegradability, and cell surface recognition sites.[11] Polysaccharides such as dextran, chitosan, cellulose, and starch have a large number of reactive groups and controllable molecular weight, contributing to their diversity in structure and property for intended use.[12] Specifically, dextran has been used clinically for more than five decades as plasma volume expansion, peripheral flow promotion, and antithrombolytic agents.[13]

From the viewpoint of polyelectrolytes, polysaccharides can be divided into polyelectrolytes like chitosan and nonpolyelectrolytes like dextran. A great number of chitosan-based nanoparticles including micelles have been studied for drug delivery.[14,15] With the progress of time, more polysaccharide-based nanoparticles enrich the versatility of drug carriers in terms of category and function. Dextran consists mainly of linear α-1,6-glucosidic linkage and has no surface charge.[16] It has been proved that positively charged drug delivery systems could form aggregates in the presence of negatively charged serum proteins once administrated intravenously.[17] The drug delivery systems without surface charge could reduce plasma protein adsorption and increase the rate of nonspecific cellular uptake.[18]
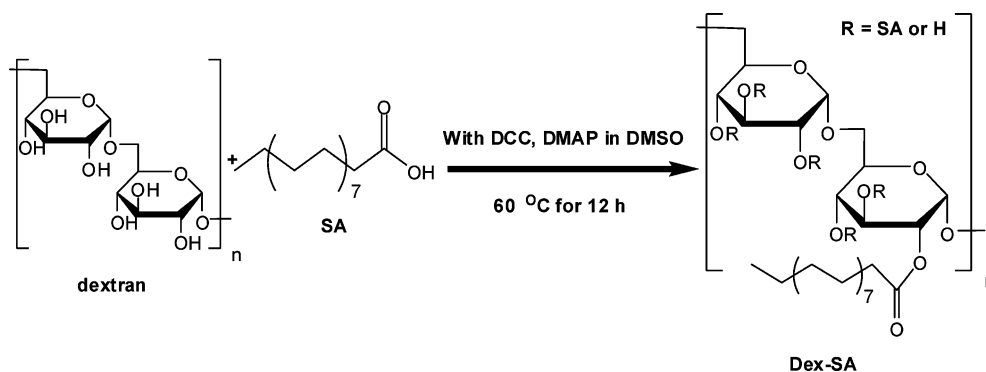
The anthracycline anticancer drug, doxorubicin (DOX), is widely used in chemotherapy for various tumors, including hematological malignancies, many types of carcinoma, and soft tissue sarcomas. However, its toxicity in normal tissue and pervasive cardiotoxic effects limits its clinical ap-

Scheme 1. Synthetic scheme of Dex-SA

plication.[19] Moreover, anthracycline anticancer drugs have been proven to be P-Glycoprotein (P-gp) substrates.[20] P-gp could efflux toxic reagent out of tumor cells, contributing to multiple drug resistance (MDR) in tumor cells.[21] Using polymeric micelles as drug delivery systems might reverse MDR.[22] Recently, Susa et al. used a lipid-modified dextran-based polymeric nanosystem for doxorubicin loading[23] and siRNA delivery.[24] This nanosystem showed pronounced antiproliferative effects against osteosarcoma cell lines and had potential for reversing MDR in osteosarcoma.

In this contribution, stearate-grafted dextran (Dex-SA) was synthesized successfully *via* an esterification reaction. Stearic acid (SA) is an endogenous saturated fatty acid and biocompatible with low toxicity and favored by pharmaceutical use.[25,26] By controlling the molecular weight of Dex and the feeding amount of SA, various Dex-SAs were synthesized, and the self-assembly behavior was investigated. Using DOX as a model anticancer drug, DOX-loaded Dex-SA micelles were prepared. The measures of the performance of Dex-SA micelle as a drug delivery carrier such as drug-loading ability, *in vitro* drug release behavior, *in vitro* and *in vivo* anticancer activities were investigated in detail.

RESULTS AND DISCUSSION

Synthesis and Characterization of Dex-SA. Stearate-*g*-dextran (Dex-SA) was successfully synthesized by esterification between the carboxyl group of SA and the hydroxyl group of Dex. The synthesis route is presented in Scheme 1. Dex-SAs were synthesized by changing the molecular weight of Dex and the feeding amount of SA. The physicochemical properties of synthesized Dex-

SAs are shown in Table 1. Dex-SA with 10 kDa molecular weight of Dex and 20% feeding amount of SA is labeled as Dex(10k)-SA(20%), and the other Dex-SAs are represented in the same manner.

^{1}H NMR spectrum was used to confirm the binding between SA and Dex. ^{1}H NMR spectra of Dex, Dex-SA and SA are shown in Figure 1. The proton peak of methyl of SA (at about 0.9 ppm) was observed in ^{1}H NMR spectrum of Dex-SA (Figure 1C), while the proton peak of carboxyl of SA (at about 12.0 ppm) disappeared.

The IR spectra of Dex ($M_w = 10$ kDa), Dex(10k)-SA(30%), and SA are also shown in Figure 1. The IR spectrum of SA exhibited the characteristic absorption band at 1700 cm^{-1} due to the C=O stretching vibration of the carboxylic groups. After SA was grafted onto Dex, Dex-SA showed a peak at 1722 cm^{-1} for C=O stretching of ester groups, which was absent in dextran. The absorbance at 1655 cm^{-1} is due to the H−O−H (hydrogen bonding) group in Dex.

The graft ratio of SA which was defined as the number of SA per D-glucose units was calculated by the proton peak areas of methyl of SA (at about 0.9 ppm) and the proton peak areas of Dex (at about 4.9 ppm) in the ^{1}H NMR spectrum of Dex-SA. Table 1 indicates the graft ratio of SA increased with the increasing molecular weight of Dex or feeding amount of SA. The thermogravimetric analysis results indicated SA modification had no obvious effects on the thermal stability of Dex. This may be due to the lower SA graft ratio. Notice the graft ratios of SA of synthesized Dex-SA (Table 1) were lower than 7.65%.

The synthesized Dex-SAs could easily self-assemble to form micelles in aqueous medium. The critical mi-

TABLE 1. Physicochemical properties of synthesized Dex-SA^a

type of Dex-SA	graft ratio (%)	CMC (mg mL^{-1})	d_n (nm)	PI (−)
Dex(10k)-SA(20%)	1.45	0.08	51.03 ± 8.73^b	0.21 ± 0.05
Dex(10k)-SA(30%)	6.33	0.01	18.30 ± 0.92	0.30 ± 0.06
Dex(20k)-SA(10%)	1.93	0.05	75.23 ± 17.55^c	0.31 ± 0.10
Dex(20k)-SA(20%)	3.86	0.02	42.32 ± 8.23	0.53 ± 0.05
Dex(20k)-SA(30%)	6.60	0.01	34.80 ± 16.55^c	0.29 ± 0.11
Dex(40k)-SA(20%)	7.65	0.01	81.17 ± 8.11^b	0.33 ± 0.04

$^a d_n$ and PI present hydrodynamic diameter and polydispersity index of micelles, respectively. Data represent the mean ± standard deviation ($n = 3$). $^b p < 0.05$. $^c p < 0.05$.
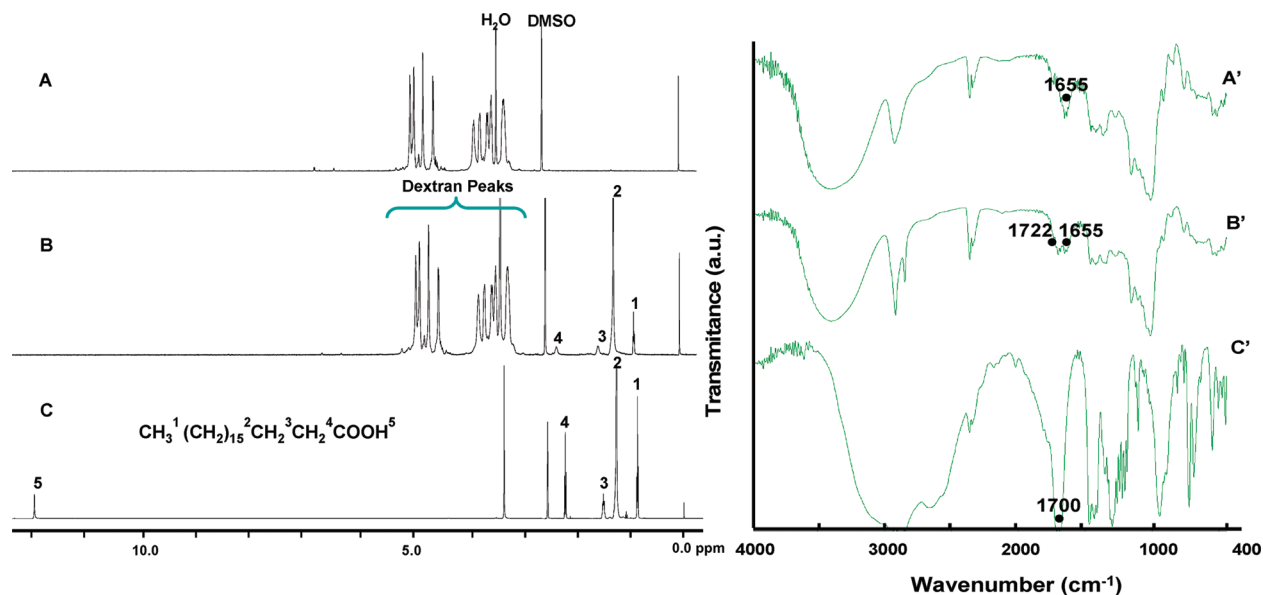
Figure 1. ^{1}H NMR spectra and FTIR spectra: (A and A′) Dex (M_w = 10 kDa); (B and B′) Dex(10k)-SA(30%); (C and C′) SA.

celle concentration (CMC) is an important characteristic for amphiphilic materials, indicating the micelle formation ability. The aggregation behavior of Dex-SA was investigated by fluorometry using pyrene as a probe. Figure 2 shows the variation of fluorescence intensity ratio for I_1/I_3 against the logarithm of Dex(10k)-SA(30%) concentration. With the lower Dex(10k)-SA (30%) concentration, the ratio of the first peak to the third peak (I_1/I_3) in the emission spectra of pyrene kept constant. As Dex(10k)-SA (30%) concentration increased to form micelles, the incorporation of pyrene into the micelles resulted in the increase of fluorescence intensity. The I_3 of pyrene increased significantly faster than that of I_1. As a result, the value of I_1/I_3 deceased sharply, indicating micelle formation. Table 1 shows that the CMC value is reduced with the increasing graft ratio of SA.

In the previous research, chitosan derivate with glycolipid-like composition, stearate-g-chitosan oligosaccharide (CSO-SA), was synthesized by the coupling reaction between the amino group of CSO and the carboxyl group of SA.[27] The derivate could self-
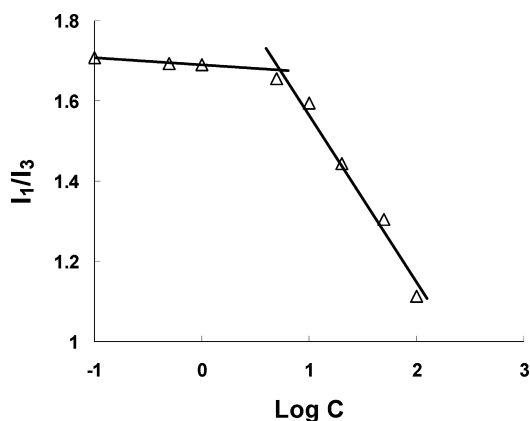
assemble to form micelles in aqueous medium, and presented fast internalization into tumor cells due to the spatial structure with multi hydrophobic core. CSO with protonated amines formed a hydrophilic shell while most SA chains aggregated into a hydrophobic core and residuary SA formed "minor cores" (hydrophobic microdomains) near the surface of the shell due to the stereo resistance effect from the shell. The synthesized Dex-SA in this research could also easily self-aggregate to form micelles in aqueous medium. A relatively lower CMC value (below 0.08 mg mL^{-1}) than that of CSO-SA might be attributed by the neutral property of Dex. The low CMC meant that Dex-SA could easily form micelles and keep the core–shell structure even under highly diluted conditions. Moreover, the CMC value decreased with the increasing graft ratio of SA. It could be explained that, when the molecular weight of the hydrophilic block exceeded that of the hydrophobic block, the polymers could disperse easily in water and form micelles.[28]

Preparation and Characteristics of Blank and DOX-Loaded Micelles. Table 1 shows the micellar hydrodynamic diameter and polydispersity index of Dex-SA micelles in pure water. The hydrodynamic diameter reduced with the increasing graft ratio of SA or the decreasing molecular weight of Dex. Physicochemical properties of DOX-loaded Dex-SA (Dex-SA/DOX) micelles are shown in Table 2. It was clear that the hydrodynamic diameter was larger after loading the drug.

Figure 3 shows the size distribution obtained by DLS (dynamic light scattering) and TEM (transmission electron microscopy) images of blank and DOX-loaded Dex(10k)-SA(30%) micelles. Their spherical morphology can be observed (Figure 3C, D). The micellar size observed in TEM images corresponded to that obtained from DLS determination, both below 50 nm.

Figure 2. Variation of intensity ratio (I_1/I_3) *versus* logarithm of Dex(10k)-SA(30%) concentration.

TABLE 2. Characteristics of DOX-loaded Dex-SA micelles[a]

type of Dex-SA	DOX: Dex-SA(w/w, %)	d_n (nm)	PI (—)	DL (%)	EE (%)
Dex(10k)-SA(20%)	10	155.25 ± 43.63	0.34 ± 0.02	3.84 ± 0.43	39.73 ± 5.41
Dex(10k)-SA(30%)	5	24.65 ± 6.16	0.72 ± 0.07	4.41 ± 0.02	92.23 ± 0.43
	10	29.10 ± 8.34	0.34 ± 0.03	8.13 ± 0.65	88.54 ± 7.71
	20	37.00 ± 2.69	0.50 ± 0.05	14.41 ± 0.83	84.25 ± 5.66
Dex(20k)-SA(10%)	10	258.30 ± 38.89	0.55 ± 0.08	3.69 ± 1.04	38.03 ± 10.97
Dex(20k)-SA(20%)	10	229.60 ± 26.16	0.41 ± 0.05	4.35 ± 1.17	45.65 ± 12.83
Dex(20k)-SA(30%)	10	148.70 ± 8.34	0.39 ± 0.08	5.33 ± 1.17	56.19 ± 13.34
Dex(40k)-SA(20%)	10	188.17 ± 25.38	0.31 ± 0.05	5.18 ± 0.83	54.47 ± 9.42

[a]d_n and PI present hydrodynamic diameter and polydispersity index of micelles, respectively. Data represent the mean ± standard deviation ($n = 3$).

DOX-loading capacities of Dex-SA micelles were affected by the properties of Dex-SA, such as the graft ratio of SA and the molecular weight of Dex (Table 2). Without calculating the drug loss in preparation, more than 99% of DOX was encapsulated into Dex-SA micelles in the final Dex-SA/DOX solution (data not shown). However, the drug loss was considered for the EE% as shown in Table 2. The Dex(10k)-SA(30%) micelle had the highest drug-loading capacity. When the DOX feeding amount was enhanced from 5% to 20%, both the DL% and EE% of Dex(10k)-SA(30%)/DOX increased consequently.

In vitro drug release profiles of Dex-SA/DOX micelles in pH 7.4 phosphate-buffered saline (PBS) are shown in Figure 4. The drug release rate was affected by the composition of Dex-SA or DOX content. As shown in Figure 4A,B, drug release rate was delayed as the graft ratio of SA or the molecular weight of Dex was enhanced. Dex-SA/DOX micelles with different drug content also showed a significant difference in drug release behavior (Figure 4C). The lower drug release rate

was found in Dex-SA/DOX micelles with higher DOX content. An *in vitro* drug release test was also conducted using PBS solution containing 10% fetal bovine serum as dissolution medium (Figure 4C). No obvious change in drug release behavior was found in the presence of serum.

Owing to the much larger molecular weight of Dex compared with that of SA, Dex-SA micellar size was below 100 nm. Furthermore, the micellar size was also affected by the hydrophobic content, graft ratio of SA. As shown in Table 1, Dex-SA micelles with higher graft ratios had smaller micellar size, which might result from the increasing hydrophobic interaction among SA chains. For the same reason, the Dex-SA micelles with higher graft ratios of SA consequently had relatively higher drug encapsulation efficiency (Table 2).

In Figure 4A,B, the drug release rate from Dex(20k)-SA(30%)/DOX and Dex(40k)-SA(20%)/DOX was slower, although the Dex(20k)-SA(30%)/DOX and Dex(40k)-SA(20%)/DOX micelles had smaller size. The micellar size is a key factor affecting the surface area making contact with the dissolution medium: the larger the area, the faster the drug release.[27] The inconsistent results meant the drug release rate was probably dominated by the increasing interaction among hydrophobic SA chains and DOX in this case. In Figure 4C, the drug release rate of Dex(10k)-SA(30%)/DOX with 20% DOX feeding amount was slower, mainly affected by particle size.

Cellular Uptake Studies. The cellular uptake test by A549 (human lung adenocarcinoma cell line) cells was carried out using FITC (fluorescein isothiocyanate)-labeled Dex(10k)-SA(30%)/DOX. Figure 5 presents the images of A549 cells after incubation with FITC-labeled Dex(10k)-SA(30%)/DOX for 2 and 24 h. The green fluorescence indicates the FITC-labeled Dex-SA micelles inside cells (Figure 5C, C′). The results demonstrated the Dex-SA/DOX micelles had excellent time-dependent cellular uptake ability. The red fluorescence indicates the DOX inside the cells (Figure 5D, D′). It was clear that DOX could be accumulated into cells mediated by Dex-SA micelles.

In Vitro **Antitumor Activity.** Cytotoxicities of DOX · HCl, blank, and DOX-loaded Dex(10k)-SA(30%) micelles against A549 (human lung adenocarcinoma cell line), MCF-7 (human breast carcinoma cell line), and MCF-7/
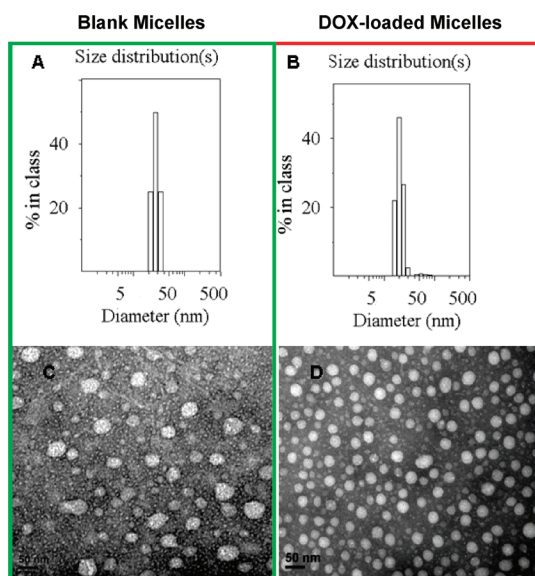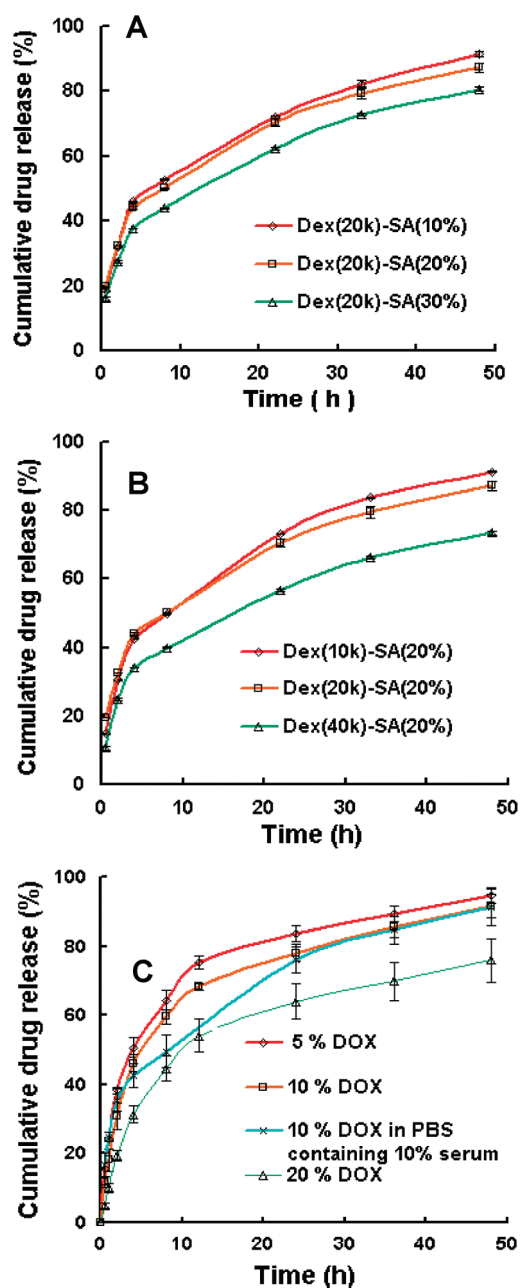

Figure 3. Size distribution obtained by DLS and TEM images of blank and DOX-loaded Dex(10k)-SA(30%) micelles: (A) Size distribution of blank Dex(10k)-SA(30%) micelles. (B) Size distribution of DOX-loaded Dex(10k)-SA(30%) micelles. (C) TEM image of blank Dex(10k)-SA(30%) micelles. (D) TEM image of DOX-loaded Dex(10k)-SA(30%) micelles.

6897

Figure 4. *In vitro* drug release profiles of Dex-SA/DOX micelles in pH 7.4 PBS at 37 °C: (A) With the same molecular weight (20 kDa) of Dex and different SA charged amounts: 10%, 20%, and 30%. (B) With the same SA charged amount (20%) and different molecular weight of Dex: 10, 20, and 40 kDa. (C) Dex(10k)-SA(30%)/DOX micelles prepared using 5%, 10%, and 20% by weight charged ratio of DOX to Dex-SA, and Dex(10k)-SA(30%)/DOX micelles prepared 10% weight charged ratio of DOX to Dex-SA in pH 7.4 PBS containing 10% fetal bovine serum.

Adr (multidrug resistant human breast carcinoma cell line) cells were investigated. Using the MTT method, the 50% cellular growth inhibitions (IC_{50}) within 48 h were determined. The IC_{50} values of blank Dex(10k)-SA(30%) micelles in model cells were determined as 200−400 $\mu g\ mL^{-1}$, indicating that the present micelles had relatively low cytotoxicity. MCF-7/Adr cells were DOX resistant, and the IC_{50} value of DOX·HCl was about 25-fold
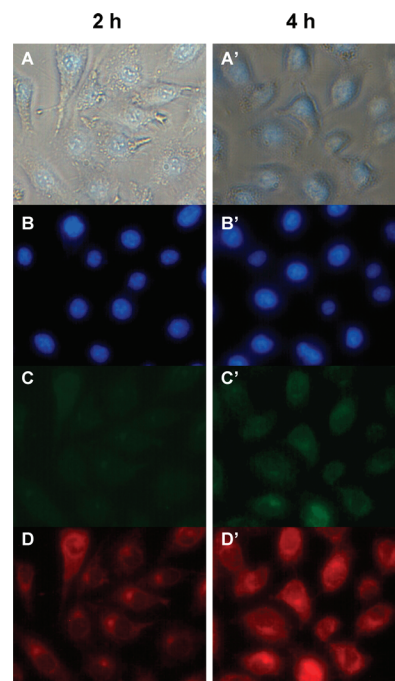
Figure 5. Images after A549 cells were incubated with FITC-Dex(10k)-SA(30%)/DOX micelles solution for 2 and 24 h, respectively. (A, A′) Phase-contrast images of cells. (B, B′) Blue fluorescence images of Hoechst staining to cells nucleus. (C, C′) Green fluorescence images of FITC labeled micelles. (D, D′) Red fluorescence images of DOX.

higher than that against drug-sensitive MCF-7 cells. As shown in Figure 6, Dex(10k)-SA(30%)/DOX showed similar cytotoxicities against drug-sensitive A549 and MCF-7 cells compared with that of DOX·HCl solution, which might be due to the determination time of the *in vitro* cytotoxicity test. The DOX could not release completely from the micelles inside the cells within 48 h. However, on the drug-resistant MCF-7/Adr cells, the cytotoxicity of Dex(10k)-SA(30%)/DOX was about 10-fold higher than that of DOX·HCl solution, which was close
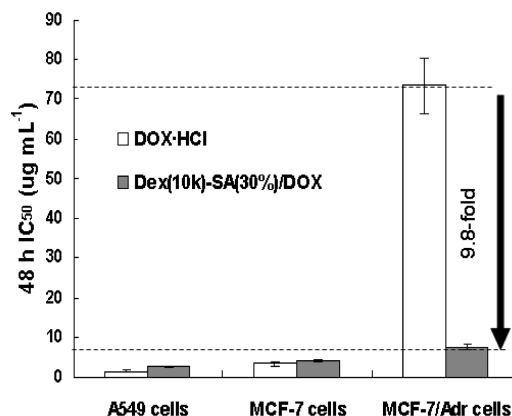
Figure 6. Comparison of IC_{50} values of DOX·HCl and Dex(10k)-SA(30%)/DOX micelles against A549, MCF-7, and MCF-7/Adr cells. Reversal power was calculated from the equation of (Rf/Sf)/(RM/Sf). Rf: IC_{50} value of drug solution against drug-resistant cells; Sf: IC_{50} value of drug solution against drug-sensitive cells; RM: IC_{50} value of Dex(10k)-SA(30%)/DOX micelles against drug-resistant cells. Data represent the mean ± standard deviation ($n = 3$).

MCF-7 cells DOX·HCl Dex(10k)-SA(30%)/DOX   **MCF-7/Adr cells** DOX·HCl Dex(10k)-SA(30%)/DOX
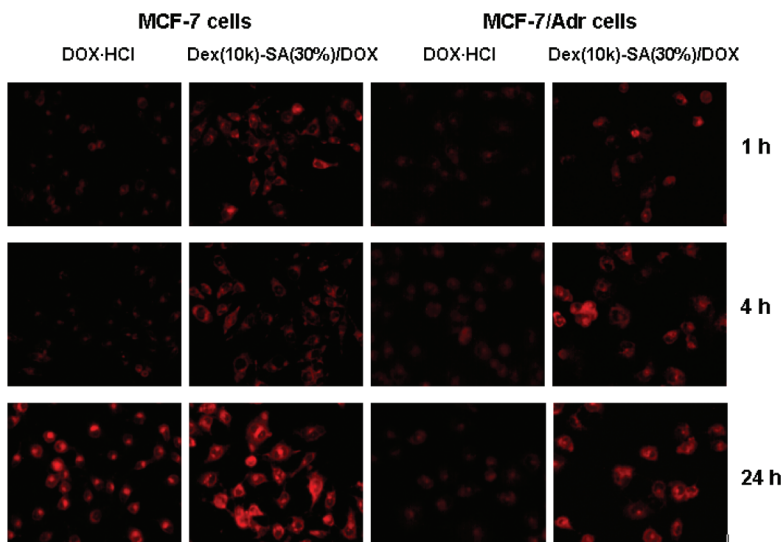
1 h

4 h

24 h

Figure 7. Fluorescence images of DOX after MCF-7 and MCF-7/Adr cells were incubated with DOX · HCl and Dex(10k)-SA(30%)/DOX micelles (both final DOX content was 4 mg mL^{-1}) for 1, 4, and 24 h, respectively.

to the value of Dex(10k)-SA(30%)/DOX micelles against drug-sensitive MCF-7 cells. The results indicated that Dex(10k)-SA(30%)/DOX micelles could reverse the DOX resistance of MCF-7/Adr cells. The reversal power of Dex(10k)-SA(30%)/DOX micelles against MCF-7/Adr cells was about 10-fold.

Figure 7 indicates the cellular images after the MCF-7 and MCF-7/Adr cells were incubated with DOX·HCl and Dex(10k)-SA(30%)/DOX micelles for 1, 4, and 24 h. The cellular uptake of DOX·HCl by drug-resistant MCF-7/Adr cells reduced significantly compared with that by drug-sensitive MCF-7 cells. However, cellular uptake of Dex-SA/DOX micelles by MCF-7/Adr cells was close to that of MCF-7 cells. Cell membrane is naturally impermeable to complexes with molecular weights larger than 1 kDa.[29] DOX molecular weight is 543.52 Da and Dex(10k)-SA(30%)/DOX micelle is over 10 kDa. The free DOX·HCl molecule could internalize into tumor cells with molecular diffusion mechanism. After DOX loaded into Dex-SA micelles, the cellular uptake mechanism might be endocytosis, which was also an efficient route for drugs going through cell membrane.[22] It was worthwhile to notice that red fluorescence of DOX was observed in the cell nucleus. As we know, the action mechanism of DOX is to intercalate DNA and RNA in the nucleus. The Dex-SA micelles could enhance the cytoplasmic and nucleus localization of DOX, which facilitated the antitumor efficacy of DOX.

P-Glycoprotein (P-gp), a kind of ATP-binding cassette (ABC) transporter expressed on the cell membrane, may contribute to drug resistance in cancer as a result of effluxing out the chemotherapeutic agents through ATP-dependent transport. Dex-SA/DOX micelles might enter into cells *via* endocytosis, which is also ATP dependent but not P-gp dependent. The endocytosis of Dex-SA/DOX micelles consumed ATP,

which consequently reduced the activity of energy-driven P-gp.[30,31] Besides, the sustained DOX released from micelles in cytoplasma and nucleus also suppressed the P-gp action.[32] As a result, against the drug-resistant MCF-7/Adr cells, the cytotoxicity of Dex(10k)-
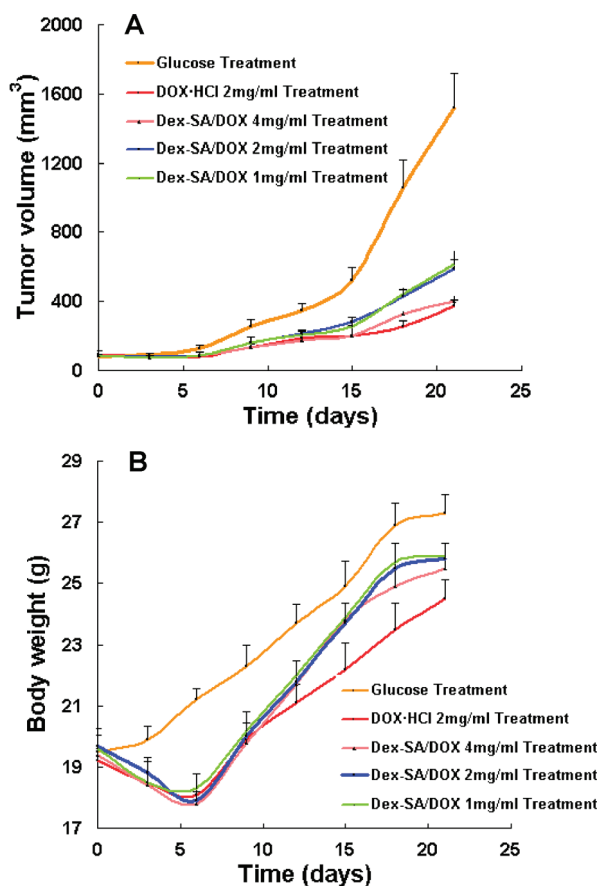

Figure 8. *In vivo* antitumor activities of Adriamycin and Dex(10k)-SA(30%)/DOX micelles after i.v. injection in the tail of tumor-bearing nude mice: (A) Mice tumor volume changes within 21 d. (B) mice body weight changes within 21d. Data represent the mean ± standard deviation (*n* = 6).

SA(30%)/DOX was about 10-fold higher than that of DOX · HCl solution.

In Vivo Antitumor Activity. Adriamycin (a commercial doxorubicin hydrochloride injection) and Dex(10k)-SA(30%)/DOX micelles solution were injected through the tail vein into nude mice bearing A549 human lung adenocarcinoma. The changes in the tumor volume were plotted (Figure 8A).Both Adriamycin and Dex(10k)-SA(30%)/DOX treatments effectively suppressed tumor growth. After i.v. injection for 9 days, tumor volumes of nude mice treated with Adriamycin and Dex(10k)-SA(30%)/DOX micelles were significantly smaller than those treated with glucose. P [Adriamycin 2 mg kg^{-1} treatment] < 0.001, P [Dex(10k)-SA(30%)/DOX 4 mg kg^{-1} treatment) < 0.001. P [Dex(10k)-SA(30%)/DOX 2 mg kg^{-1} and 1 mg kg^{-1} treatments) < 0.05, after 12 days, P [Dex(10k)-SA(30%)/DOX 2 mg kg^{-1} and 1 mg kg^{-1} treatments) < 0.001. After 18 days, the tumor volumes treated with Adriamycin (2 mg kg^{-1}) were significantly smaller than those treated with Dex(10k)-SA(30%)/DOX (2 mg kg^{-1} and 1 mg kg^{-1}) ($p < 0.001$) but not significantly different from those treated with Dex(10k)-SA(30%)/DOX (4 mg kg^{-1}) ($p > 0.05$). As shown in Figure 8B, continuous increase of the body weight in all groups indicated that all the doses were within the safe range.

The tumor inhibition rate of Adriamycin (2 mg kg^{-1}) was 79.73%, Dex(10k)-SA(30%)/DOX (4 mg kg^{-1}) was 81.08%, Dex(10k)-SA(30%)/DOX (2 mg kg^{-1}) was 81.80%, Dex(10k)-SA(30%)/DOX (1 mg kg^{-1}) was 73.87%. All the tumor inhibition values larger than 40% were considered to be effective treatment. The tumor inhibition rate with treatment with Dex(10k)-SA(30%)/DOX increased with the enhanced dose. There was no significant difference between the tumor inhibition rates of those treated with the same dose ($p > 0.05$) of Dex(10k)-SA(30%)/DOX and of Adriamycin. However, the body weight of mice administrated with Dex(10k)-SA(30%)/DOX (4 mg kg^{-1}) after 21 d was significantly greater than that of mice treated with Adriamycin (2 mg kg^{-1}) ($p < 0.05$). The mice administrated with Adriamycin (4 mg kg^{-1}) died, while the ones administrated with Dex-SA/DOX (6 mg kg^{-1}) survived. It indicated that Dex-SA/DOX micelles could reduce toxicity to normal tissues as remaining therapeutic effects.

CONCLUSIONS

Dex-SA was synthesized successfully with low CMC. The Dex-SA could self-assemble to form nanosized micelles in aqueous medium and indicated excellent tumor cellular uptake ability. The *in vitro* drug release from Dex-SA/DOX micelles could be prolonged for 48 h and adjusted by composition of Dex-SA and DOX content. Dex-SA/DOX micelles were effective for suppressing both drug-sensitive and drug-resistant MCF-7 cells and for reversing the drug resistance of MCF-7/Adr cells. The assay of antitumor activity *in vivo* indicated that Dex-SA/DOX micelles could reduce the toxicity to normal tissues as remaining therapeutic effects compared with commercial doxorubicin hydrochloride. Overall, the results suggested that the Dex-SA micelle was a potential candidate for drug delivery.

MATERIALS AND METHODS

Synthesis and Characterization of Dex-SA. The stearate-grafted dextran (Dex-SA) was synthesized by esterification reaction between carboxyl group of stearic acid (SA, $C_{18}H_{36}O_2$, Sigma Aldrich Co.) and the hydroxyl group of dextran (Dex, $(C_6H_{12}O_5)_n$, BIO BASIC INC.) in the presence of the coupling agent, N,N′-dicyclohexylcarbodiimide (DCC, $C_{13}H_{22}N_2$, Shanghai Medped Co.) and the catalyst, 4-dimethylaminopyridine (DMAP, $C_7H_{10}N_2$, Shanghai Medped Co.). Briefly, SA (charged ratios were 10%, 20%, and 30%, referring to the charged molar number of D-glucose units in dextran), DCC, and DMAP (SA:DCC:DMAP = 1:3:0.3, mol:mol:mol) were dissolved in 45 mL of anhydrous dimethyl sulfoxide (DMSO, Haishuo Biochemistry Co., Ltd., Wuxi, China). The solution was stirred under the protection of nitrogen for 30 min to activate the carboxylic acid of SA. After 1.0 g of Dex was added, the reaction was carried out in nitrogen gas overnight at 60 °C under stirring at 250 rpm. The reaction solution was then dialyzed (MWCO 7.0 kDa, Spectrum Laboratories, Laguna Hills, CA) against pure water for 48 h with frequent exchange of pure water. After the dialyzed solution was centrifugated at 15000 rpm (3K30, SIGMA Labrorzentrifugen GmbH, Germany) to remove DMAP and other water-insoluble byproducts, and the freeze-dried product (using LABCONCO, FreeZone 2.5 Plus, U.S.A.) was dispersed in anhydrous ethanol (Haishuo Biochemistry Co., Ltd., Wuxi, China) with the help of ultrasonicator (400 W, JY92-II, Ningbo Xinzhi Scientific Instrument Institute, Zhejiang, China) to remove unreacted SA. Finally, the precipitated product was lyophilized, and Dex-SA was received.

The composition of obtained Dex-SA was confirmed by ^{1}H NMR × spectra using a NMR spectrometer (AC-80, Bruker Bios pin. Germany). Twenty milligrams per milliliter of dextran, SA, and Dex-SA in dimethylsulfoxide-d_6 were measured. The SA graft ratio for Dex-SA (GR %) was calculated using the formula 1:

$$GR\% = A_{0.9}/(A_{4.9} \times 3) \times 100\% \qquad (1)$$

$A_{0.9}$ and $A_{4.9}$ represent the peak areas at chemical shifts at 0.9 and 4.9 ppm in the ^{1}H NMR spectrum of Dex-SA, respectively. The chemical shift at 4.9 ppm corresponded to the proton of near glucosidic linkage in glucose unit.

IR spectra were recorded on a JASCO Fourier-transform infrared spectrometer. Dex, SA, and Dex-SA were thoroughly ground with exhaustively dried KBr, and discs were prepared by compression under vacuum.

The critical micelle concentration (CMC) of Dex-SA was determined by fluorescence measurement using pyrene as a probe.[33] The excitation wavelength was set at 337 nm, the excitation slit at 2.5 nm, and the emission slit at 10 nm. The intensities of the emission at a wavelength range of 360−450 nm were monitored using a fluorescence spectrophotometer (F-2500, Hitachi Co., Japan). The concentration of Dex-SA solution was varying from 1.0×10^{-3} to 1.0 mg mL^{-1} containing 5.94×10^{-7} M of pyrene. Then the emission intensity ratio of the first peak (I_1, 374 nm) to the third peak (I_3, 385 nm) was calculated for the determination of CMC.

Preparation of Blank and DOX-Loaded Dex-SA Micelles. The blank Dex-SA micelles solution was prepared by dissolving 10 mg of Dex-SA into 10 mL of pure water using the treatment of probe-

type ultrasonicator (400 W, JY92-II, Ningbo Xinzhi Scientific Instrument Institute, Zhejiang, China) for 30 times (active every 2 s for a 3-s duration) at room temperature.

Doxorubicin base (DOX) was obtained by the reaction of DOX·HCl (Hisun Pharm Co.) with twice the molar amount of triethylamine in DMSO overnight.[34] Different volumes of 1 mg mL^{-1} DOX DMSO solution was added into Dex-SA micelles solution (DOX:Dex-SA = 5%, 10%, 20%, w/w). The mixture solution was dialyzed (MWCO 7.0 kDa) against pure water for 24 h with frequent exchange of pure water. After dialysis, the mixture solution was centrifuged at 4000 rpm for 10 min to remove drug that precipitated during the dialysis process, and the DOX-loaded Dex-SA (Dex-SA/DOX) micelles solution was obtained.

Physicochemical Properties of Blank and DOX-Loaded Dex-SA Micelles. The micellar size and size distribution were determined by dynamic light scattering using a ZETASIZER (3000HS, Malvern Co., UK).

The morphological examinations were performed by a transmission electron microscopy (TEM) (JEOL JEM-1230, Japan). The samples were dropped onto a formar-coated copper grid and stained with 2% (w/v) phosphotungstic acid for viewing.

The DOX content in micelles was determined using a fluorescence spectrophotometer (F-2500, Hitachi Co., Japan). Dex-SA/DOX micelles solution was diluted 10-fold by DMSO to dissociate the micelles, and then the fluorescence intensity was measured. The excitation wavelength was set at 505 nm, the emission wavelength at 560 nm, the excitation slit at 5.0 nm, and the emission slit at 5.0 nm. The DOX content was calculated by comparing to standard curve obtained from DOX DMSO aqueous solution (DMSO:H$_2$O = 9:1, v:v).

The DOX-loading content (DL%) and encapsulation efficiency (EE%) were calculated using eqs 2 and 3 below, respectively:

$$DL\% = \frac{\text{mass of DOX encapsulated in micelles}}{\text{mass of DOX-loaded micelles}} \times 100\% \quad (2)$$

$$EE\% = \frac{\text{mass of DOX encapsulated in micelles}}{\text{mass of DOX added}} \times 100\% \quad (3)$$

In Vitro DOX Release From Dex-SA/DOX Micelles. *In vitro* drug release experiments were conducted using the dialysis method. One milliliter of Dex-SA/DOX micelles solution was sealed in a dialysis bag (MWCO 7.0 kDa) and was immersed into 30 mL of phosphate buffer solution (PBS) at pH 7.4 (or PBS solution containing 10% fetal bovine serum) in a plastic tube. The experiments were carried out in an incubator shaker (HZ-8812S, Scientific and Educational Equipment Plant, Taicang, China) which was maintained at 37 °C and shaken horizontally at 60 rpm. The solution in the tube was periodically withdrawn and replaced with fresh PBS at predefined time intervals. DOX content in PBS was determined by a fluorescence spectrophotometer (F-2500, Hitachi Co., Japan). All drug release tests were performed thrice.

Cell Culture. A549, MCF-7, and MCF-7/Adr cells were donated by the second Affiliated Hospital, College of Medicine, Zhejiang University (Hangzhou, China). Cells were maintained in RPMI 1640 (Gibco BRL, U.S.A.) supplemented with 10% (v/v) FBS (fetal bovine serum) (Sijiqing Biologic, Hangzhou, China) and penicillin/streptomycin (100 U mL^{-1}, 100 U mL^{-1}) at 37 °C in a humidified atmosphere containing 5% CO$_2$. Cells were subcultured regularly using trypsin/EDTA.

Cellular Uptake of DOX-Loaded Dex-SA Micelles. FITC-labeled Dex-SA micelles were prepared by adding 2.0 mg mL^{-1} FITC (C$_{21}$H$_{11}$NO$_5$S, Sigma Chemical Co.) ethanol solution into 1.0 mg mL^{-1} Dex-SA aqueous solution (Dex-SA:FITC = 1:8, mol:mol). The mixture solution was stirred in aphotic environment for 24 h and then was dialyzed (MWCO 7.0 kDa) against pure water overnight with frequent exchange of pure water to remove ethanol and unreacted FITC. Finally, FITC-Dex-SA micelles solution was obtained. Then the DOX-loaded micelles were prepared using the FITC-labeled Dex-SA for the cellular uptake test.

The cells were seeded at 10^5 mL^{-1} cells/well in a 24-well plate (Nalge Nunc International, Naperville, IL, U.S.A.) and incubated for 24 h. Then the cells were exposed to a medium containing DOX·HCl or FITC-labeled Dex-SA/DOX micelles for further incubation. After washing the cells with PBS three times, the cellular uptake was observed using a fluorescence microscope (Olympus America, Melville, NY, U.S.A.).

Cytotoxicity Evaluation. Cytotoxicities of DOX·HCl, blank, and DOX-loaded Dex-SA micelles against A549, MCF-7, and MCF-7/Adr were evaluated by MTT assay. In a 96-well culture plate (Nalge Nunc International, Naperville, IL, U.S.A.) were seeded 10^4 cells/well and incubated for 24 h. After preincubation, cells were exposed to DOX·HCl, blank, and DOX-loaded Dex-SA micelles solution with serial concentrations for 48 h. At predetermined times, 15 μL of 3-(4,5-dimethylthiazol-2-yl)-2,5-diphenyltetrazolium bromide (MTT) (C$_{18}$H$_{16}$BrN$_5$S, Sigma Chemical Co.) solution with the concentration of 5 mg mL^{-1} was added and incubated for further 4 h. Then the metabolized product, MTT formazan was dissolved by 200 μL of DMSO into each well. Finally, the plates were shaken for 20 min, and the absorbance of the formazan product was measured at 570 nm in a microplate reader (Bio-Rad, model 680, U.S.A.).

In Vivo **Antitumor Activity of DOX-Loaded Dex-SA Micelles.** All animal procedures were approved by the Zhejiang University Institutional Animal Care and Use Committee. BALB/C+nu/F1 nude mice 6−8 weeks old were transplanted with A549 cells and drug injection *via* tail vein was started when the tumor volume reached approximately 100 mm^3. Mice were divided into five groups, six mice in each group. The first group, as control, was injected with 0.2 mL of glucose solution for 7 days consecutively. The second group was injected with 2 mg kg^{-1} body weight of Adriamycin (commercial doxorubicin hydrochloride injection) for 7 days consecutively. The third, fourth, and fifth groups were injected with Dex-SA/DOX micelles, 1 mg of equivalent DOX kg^{-1}, 2 mg of equivalent DOX kg^{-1}, and 4 mg of equivalent DOX kg^{-1}, respectively, for 7 days consecutively.

The size of the tumor and the body weight of each mouse were monitored every 3 days thereafter. After 21 days, the nude mice were sacrificed, and the tumor weight was measured.

Tumor volume and inhibition of tumor growth (%) were respectively calculated using the eqs 4 and 5 below:

$$\text{tumor volume} = \frac{(\text{the smallest diameter}) \times (\text{the smallest diameter}) \times (\text{the largest diameter})}{2} \quad (4)$$

$$\text{inhibition of tumor growth (\%)} = 1 - \frac{(\text{the average tumor weight of treated group})}{(\text{the average tumor weight of controlled group})} \times 100\% \quad (5)$$

Statistical Analysis. Data were expressed as means of three or six separate experiments and were compared by *t* tests. A *P*-value <0.05 was considered statistically significant in all cases.

Supporting Information Available: Thermogravimetric analysis and results of the Dex-SA. This material is available free of charge *via* the Internet at http://pubs.acs.org.

REFERENCES AND NOTES

1. Matsumura, Y.; Maeda, H. A New Concept for Macromolecular Therapeutics in Cancer-Therapy-Mechanism of Tumoritropic Accumulation of Proteins and the Antitumor Agent Smancs. *Cancer Res.* **1986**, *12*, 6387–6392.
2. Li, S. D.; Huang, L. Pharmacokinetics and Biodistribution of Nanoparticles. *Mol. Pharm.* **2008**, *5*, 496–504.

3. Adams, M. L.; Lavasanifar, A.; Kwon, G. S. Amphiphilic Block Copolymers for Drug Delivery. *J. Pharm. Sci.* **2003**, *92*, 1343–1355.

4. Shuai, X. T.; Merdan, T.; Schaper, A. K.; Xi, F.; Kissel, T. Core-Cross-Linked Polymeric Micelles as Paclitaxel Carriers. *Bioconjugate Chem.* **2004**, *15*, 441–448.

5. Xie, J. W.; Wang, C. H. Self-Assembled Biodegradable Nanoparticles Developed by Direct Dialysis for the Delivery of Paclitaxel. *Pharm. Res.* **2005**, *22*, 2079–2090.

6. Suh, H. R.; Jeong, B. M.; Rathi, R.; Kim, S. W. Regulation of Smooth Muscle Cell Proliferation Using Paclitaxel-Loaded Poly(ethylene oxide)poly(lactide/glycolide) Nanospheres. *J. Biomed. Mater Res.* **1998**, *42*, 331–338.

7. Kim, S. Y.; Lee, Y. M. Taxol-loaded Block Copolymer Nanospheres Composed of Methoxy Poly(ethylene glycol) and Poly(ε-caprolactone) as Novel Anticancer Drug Carriers. *Biomaterials* **2001**, *22*, 1697–1704.

8. Zhang, X. C.; Jackson, J. K.; Burt, H. M. Development of Amphiphilic Diblock Copolymers as Micellar Carriers of Taxol. *Int. J. Pharm.* **1996**, *132*, 195–206.

9. Burt, H. M.; Zhang, X. C.; Toleikis, P.; Embree, L.; Hunter, W. L. Development of Copolymers of Poly(D,L-lactide) and Methoxypolyethylene Glycol as Micellar Carriers of Paclitaxel. *Colloids Surf. B.* **1999**, *16*, 161–171.

10. Deng, L. D.; Li, A. G.; Yao, C. M.; Sun, D. X.; Dong, A. J. Methoxy Poly(ethylene glycol)-*b*-poly(L-lactic acid) Copolymer Nanoparticles as Delivery Vehicles for Paclitaxel. *J. Appl. Polym. Sci.* **2005**, *98*, 2116–2122.

11. Abdurrahmanoglu, S.; Firat, Y. Synthesis and Characterization of New Dextran-acrylamide Gels. *J. Appl. Polym. Sci.* **2007**, *106*, 3565–3570.

12. Liu, Z. H.; Jiao, Y. P.; Wang, Y. F.; Zhou, C. R.; Zhang, Z. Y. Polysaccharides-Based Nanoparticles as Drug Delivery Systems. *Adv. Drug Delivery Rev.* **2008**, *60*, 1650–1662.

13. Thoren, L. The Dextrans - Clinical Data. *Dev. Biol. Stand.* **1981**, *48*, 157–167.

14. Janes, K. A.; Calvo, P.; Alonso, M. J. Polysaccharide Colloidal Particles as Delivery Systems for Macromolecules. *Adv. Drug Delivery Rev.* **2001**, *47*, 83–97.

15. Prabaharan, M.; Mano, J. F. Chitosan-Based Particles as Controlled Drug Delivery Systems. *Drug Delivery* **2005**, *12*, 41–57.

16. Larsen, C. Dextran Prodrugs-structure and Stability in Relation to Therapeutic Activity. *Adv. Drug Delivery Rev.* **1989**, *3*, 103–154.

17. Zhang, J. S.; Liu, F.; Huang, L. Implications of Pharmacokinetic Behavior of Lipoplex for Its Inflammatory Toxicity. *Adv. Drug Delivery Rev.* **2005**, *57*, 689–698.

18. Alexis, F.; Pridgen, E.; Molanr, L. K.; Farokhzad, O. C. Factors Affecting the Clearance and Biodistribution of Polymeric Nanoparticles. *Mol. Pharm.* **2008**, *5*, 505–515.

19. Barry, E.; Alvarez, J. A.; Scully, R. E.; Miller, T. L.; Lipshultz, S. E. Anthracycline-Induced Cardiotoxicity: Course, Pathophysiology, Prevention and Management. *Expert Opin. Pharmacother.* **2007**, *8*, 1039–1058.

20. Lum, B. L.; Gosland, M. P.; Kaubisch, S.; Sikic, B. I. Molecular Targets in Oncology: Implications of the Multidrug Resistance Gene. *Pharmacotherapy* **1993**, *13*, 88–109.

21. Tijerina, M.; Fowers, K. D.; Kopeckova, P.; Kopecek, J. Chronic Exposure of Human Ovarian Carcinoma Cells to Free or HPMA Copolymer-Bound Mesochlorine$_6$ Does Not Induce P-Glycoprotein-Mediated Multidrug Resistance. *Biomaterials* **2000**, *21*, 2203–2210.

22. Elamanchili, P.; Mceachern, C.; Burt, H. Reversal of Multidrug Resistance by Methoxypolyethylene Glycol−Block−Polycaprolactone Diblock Copolymers Through the Inhibition of P-Glycoprotein Function. *J. Pharm. Sci.* **2009**, *98*, 945–958.

23. Susa, M.; Iyer, A. K.; Ryu, K.; Hornicek, F. J.; Mankin, H.; Amiji, M. M.; Duan., Z. Doxorubicin Loaded Polymeric Nanoparticulate Delivery System to Overcome Drug Resistance in Osteosarcoma. *BMC Cancer* **2009**, *9*, 399.

24. Susa, M.; Iyer, A. K.; Ryu, K.; Choy, E.; Hornicek, F. J.; Mankin, H.; Milane, L.; Amiji, M. M.; Duan., Z. Inhibition of ABCB1 (MDR1) Expression by an siRNA Nanoparticulate Delivery System to Overcome Drug Resistance in Osteosarcoma. *PLoS One* **2010**, *5*, e10764.

25. Hu, F. Q.; Jiang, S. P.; Du, Y. Z.; Yuan, H.; Ye, Y. Q.; Zeng, S. Preparation and Characterization of Stearate Nanostructured Lipid Carriers by Solvent Diffusion Method in an Aqueous System. *Colloids Surf., B* **2005**, *45*, 167–173.

26. Zhang, Q. N.; Yie, G. Q.; Li, Y.; Yang, Q. S.; Nagai, Y. T. Studies on the Cyclosporin A Loaded Stearate Nanoparticles. *Int. J. Pharm.* **2000**, *200*, 153–159.

27. Hu, F. Q.; Liu, L. N.; Du, Y. Z.; Yuan, H. Synthesis and Antitumor Activity of Doxorubicin Conjugated Stearate-*g*-Chitosan Oligosaccharide Polymeric Micelles. *Biomaterials* **2009**, *30*, 6955–6963.

28. Letchford, K.; Burt, H. A Review of the Formation and Classification of Amphiphilic Block Copolymer Nanoparticulate Structures: Micelles, Nanospheres, Nanocapsules and Polymersomes. *Eur. J. Pharm. Biopharm.* **2007**, *65*, 259–269.

29. Bareford, L. A.; Swaan, P. W. Endocytic Mechanisms for Targeted Drug Delivery. *Adv. Drug Delivery Rev.* **2007**, *59*, 748–758.

30. Omelyanenko, V.; Kopeckova, P.; Gentry, C.; Kopecek, J. Targetable HPMA Copolymer Adriamycin Conjugates: Recognition, Internalization, and Subcellular fate. *J. Controlled Release* **1998**, *53*, 25–37.

31. Kabanov, A. V.; Batrakova, E. V.; Alakhov, V. Y. Pluronic Block Copolymers for Overcoming Drug Resistance in Cancer. *Adv. Drug Delivery Rev.* **2002**, *54*, 759–779.

32. Zheng, C.; Qiu, L. Y.; Yao, X. P.; Zhu, K. J. Novel Micelles From Graft Polyphosphazenes as Potential Anti-Cancer Drug Delivery Systems: Drug Encapsulation and in Vitro Evaluation. *Int. J. Pharm.* **2009**, *373*, 133–140.

33. Slaughter, J. N.; Schmidt, K. M.; Byram, J. L.; Mecozzi, S. Synthesis and Self-Assembly Properties of a Novel [Poly(ethylene glycol)]−fluorocarbon−phospholipid Triblock Copolymer. *Tetrahedron Lett.* **2007**, *48*, 3879–3882.

34. Kohori, F.; Yokoyama, M.; Sakai, K.; Okanob, T. Process Design for Efficient and Controlled Drug Incorporation into Polymeric Micelle Carrier Systems. *J. Controlled Release* **2002**, *78*, 155–163.